

Pharmacokinetics and tissue distribution of an orally administered mucoadhesive chitosan-coated amphotericin B-Loaded nanostructured lipid carrier (NLC) in rats

Janet Sui Ling Tan, Clive Roberts & Nashiru Billa

To cite this article: Janet Sui Ling Tan, Clive Roberts & Nashiru Billa (2020) Pharmacokinetics and tissue distribution of an orally administered mucoadhesive chitosan-coated amphotericin B-Loaded nanostructured lipid carrier (NLC) in rats, Journal of Biomaterials Science, Polymer Edition, 31:2, 141-154, DOI: [10.1080/09205063.2019.1680926](https://doi.org/10.1080/09205063.2019.1680926)

To link to this article: <https://doi.org/10.1080/09205063.2019.1680926>



Published online: 22 Oct 2019.



Submit your article to this journal [↗](#)



Article views: 288



View related articles [↗](#)



View Crossmark data [↗](#)



Citing articles: 12 View citing articles [↗](#)



Pharmacokinetics and tissue distribution of an orally administered mucoadhesive chitosan-coated amphotericin B-Loaded nanostructured lipid carrier (NLC) in rats

Janet Sui Ling Tan ^a, Clive Roberts ^b  and Nashiru Billa ^{a,c} 

^aSchool of Pharmacy, The University of Nottingham, Malaysia, Semenyih, Selangor, Malaysia; ^bSchool of Pharmacy, The University of Nottingham, Nottingham, UK; ^cCollege of Pharmacy, Qatar University, Doha, Qatar

ABSTRACT

Oral delivery of amphotericin B (AmpB) is desirable because it provides a more patient-friendly mode of administration compared to the current delivery approach akin with the marketed AmpB formulations. The goal of the study was to investigate the pharmacokinetics and tissue distribution of orally administered chitosan-coated AmpB-loaded nanostructured lipid carriers (ChiAmpB NLC) administered to Sprague Dawley rats at a dose of 15 mg/kg. Orally administered ChiAmpB NLC resulted in a two-fold increase in the area under the curve ($AUC_{0-\infty}$) compared to the uncoated AmpB NLC and marketed Amphotret[®]. This enhanced bioavailability of AmpB suggests prolonged transit and retention of ChiAmpB NLC within the small intestine through mucoadhesion and subsequent absorption by the lymphatic pathway. The results show that mean absorption and residence times (MAT & MRT) were significantly higher from ChiAmpB NLC compared to the other two formulations, attesting to the mucoadhesive effect. The ChiAmpB NLC presented a lower nephrotic accumulation with preferential deposition in liver and spleen. Thus, the limitations of current marketed IV formulations of AmpB are potentially addressed with the ChiAmpB NLC in addition to utilizing this approach for targeting internal organs in visceral leishmaniasis.

ARTICLE HISTORY

Received 8 July 2019
Accepted 13 October 2019

KEYWORDS

Amphotericin B; lymphatic pathway; mucoadhesion; NLC; oral delivery; pharmacokinetics; tissue distribution

Introduction

Oral administration of AmpB appeals to clinicians and patients alike because of the potential of eliminating the toxicities (notably nephrotoxicity) associated with the current mode of delivery, which is exclusively by intravenous (IV) administration. It is also bound to reduce treatment cost and improve the quality of life of the patients [1,2]. However, due to the poor solubility and permeability of AmpB, oral delivery of AmpB results in a meager bioavailability (<0.3%) which limits its therapeutic

efficacy [3,4]. Poor oral absorption of AmpB has long been reported in different animal trials such as in rats [5,6], mice [7] and dogs [8]. Nanotechnology seems to be the key to unlocking some of the constraints associated with the administration of Amp orally.

Upon oral administration, most drugs are absorbed from the small intestine to the systemic circulation *via* the portal blood vein. However, for lipid formulations or hydrophobic drugs, intestinal lymphatic pathway provides an alternative route, which bypasses the hepatic first pass metabolism at the liver and results in improved bioavailability [9–11]. Additionally, this route portrays a distinctive characteristic whereby the transportation of the drug occurs over a longer period of time compared to the portal vein route. Thus, lymphatic pathway can be exploited for prolonged delivery of therapeutic agents to the systemic circulation [12].

The goal of the this investigation was to formulate nanostructured lipid carriers (NLCs) comprised of beeswax and coconut oil as the carrier system for the oral delivery of AmpB with the aim to exploit the intestinal lymphatic pathway [13,14]. A further aim was to coat the formulation in order to impart mucoadhesive capability so that the particles are retained longer during transit in the small intestine. The delayed transit will ensure that most of the particles are taken-up. This way, the bioavailability of AmpB would be improved.

The pharmacokinetic behaviour of the marketed formulation of AmpB, Fungizone[®] administered intravenously was reported to exhibit a complex plasma profile, with a rapid fall in plasma concentration followed by a long elimination half-life (approximately 15 days). In contrast, the pharmacokinetic behaviour of orally administered AmpB is less known. It is administered orally to treat localized gastrointestinal (GI) tract infections mainly due to the poor absorption profile. It was reported that administration of high doses of AmpB (2–10 g daily) to humans resulted in similarly low plasma concentration levels as doses of 30–40 mg per day [7,15].

Tissue distribution studies on newly developed formulations is necessary since it provides information on the potential tissue accumulation of the formulation and/or the drug. Tissue accumulation thus, provides insights on potential toxicity or efficacy of the formulation. In this regard, determination of the plasma level of the AmpB alone is insufficient because there is a poor correlation between the plasma level and biodistribution of the active in the organs [16,17]. Evaluation of levels of AmpB in the kidneys is crucial because it relates to nephrotoxicity and is the major limitation to the clinical use of AmpB [15,18]. Reticuloendothelial organs (RES) such as liver and spleen are the target organs for the *Leishmania* genus, an intracellular parasite which causes high fatality if left untreated. Currently, AmpB is used as the second-line therapy for visceral leishmaniasis which comes after parental administration of pentavalent antimony organic compounds which are associated with high frequency of resistance and side effects [19]. Hence, an accumulation of the AmpB at the aforementioned sites provides an added advantage in terms of targeting strategy.

Henceforth, we aimed to evaluate the (i) pharmacokinetic profiles of AmpB from ChiAmpB NLC in comparison to uncoated AmpB NLC and the marketed formulation, Amphotret[®], (ii) retrospectively investigate the mucoadhesion behaviour of

ChiAmpB NLC *in vivo* through analyses of the levels of AmpB in the stomach and small intestine over time and (iii) investigate the tissue distribution of the AmpB in organs-of-interests; kidneys, liver and spleen.

Materials and methods

Materials

Beeswax and coconut oil were from Acros Organics, New Jersey, USA. Chitosan (low molecular weight) and phosphate buffered saline tablets (PBS) were purchased from Sigma Aldrich Co. LLC., Missouri, USA. AmpB and ethylenediaminetetracetic acid, disodium salt dihydrate (EDTA) were obtained from Fisher Scientific, India. The commercial formulation of AmpB deoxycholate (Amphotret[®], Bharat Serums and Vaccines Limited, India) was a gift from Pahang Pharmacy, Malaysia. Soya lecithin was purchased from MP Biomedicals (Illkirch, France) and acetic acid was obtained from R & M Chemicals, India. 1-amino 4-nitronaphthalene ($\geq 97\%$) was obtained from Apollo Chemicals, San Pedro Sula. All reagents and solvents used of analytical and HPLC grades respectively. Deionized water used was Milli-Q 18.2 M Ω .cm at 25 °C (Millipore Corp., Bedford, USA).

Methods

Formulation of ChiAmpB NLC formulation

The ChiAmpB NLC was formulated as recently reported [13,14]. Briefly, beeswax and coconut oil were melted at 70 °C before the addition of AmpB and at the same time, Tween-80 and lecithin were mixed with 10 mL of deionized water and stirred at 70 °C at 500 rpm for 45 min. The surfactant mixture was added into the melted lipids containing AmpB followed by homogenization at 12,400 rpm for 8 min using high speed homogenizer (Ultra-Turrax T25, Germany). The coarse emulsion was further subjected to probe ultrasonication (Q500 QSonica, Newtown, CT, USA) for further 8 min at 20% amplitude. The mixture was poured into 4 °C deionized water under 500 rpm of stirring, making up a total of 100 mL. Chitosan (dissolved in 1% v/v acetic acid) was added in a dropwise manner into the formed AmpB NLC in 1: 40 v/v under stirring of 250 rpm or 15 min.

The physical properties of the formulation were characterized in terms of particle size, polydispersity index, zeta potential, encapsulation efficiency and aggregation states as reported previously [13,14].

High performance liquid chromatography (HPLC) conditions and validation

An Agilent HPLC system (1260 Series, Waldbronn, Germany) equipped with a 15 cm \times 4.6 mm reversed-phase C-18 column, Hypersil Gold (ThermoFisher Scientific, Waltham, United States) with 5 μ m particle size stationary phase was used in this study. A mixture of 60% 2.5 mM EDTA and 40% acetonitrile was used as the mobile phase at a flow rate of 1.5 mL/min with the wavelength set at 408 nm.

Calibration curves of AmpB in plasma and tissue were established over 0.1–10 μ g/mL for plasma and 1–100 μ g/g for tissue samples, with at least six data points were

used to construct the curves. The HPLC method was further validated in terms of linearity, recovery, accuracy, precision, limit of detection (LOD) and limit of quantification (LOQ).

Animals

In this section was a probe investigation on the performance of the ChiAmpB NLC therefore, we tried to minimize the number of animals used for the study as much as possible. 12 adult male Sprague Dawley (268.4 ± 11.1 g) rats used in the pharmacokinetic and tissue distribution studies were obtained from University Putra Malaysia (UPM). The studies were carried out at The Comparative Medicine and Technology Unit (COMeT), UPM and approved by the Ethics Committee of The University of Nottingham (UNMC 19). The rats were housed in ventilated cages at ambient temperature, maintained under 12/12 light-dark cycle and supplied with food and water *ad libitum*. The rats were acclimatized for one week before the experiment, reaching the age of 8 weeks.

Drug administration and blood sampling

The rats were fasted for 12 h overnight and then divided into four groups, with three rats per group. Each group received either one of the following single dose: (i) oral gavage of AmpB NLC, (ii) ChiAmpB NLC and (iii) Amphotret[®] at 15 mg/kg of AmpB in 2 mL. The fourth group (iv) was administered 150 μ L of Amphotret[®] (IV) at a dose of 1.0 mg/kg. The rats were allowed free access to water throughout the study and food was allowed 4-hour post-dosing. The animals were slightly anaesthetized with diethyl ether at a dose of 5 g/kg prior to blood sampling. A 500 μ L aliquot of blood was collected from the tail of the rats and transferred to a Microtainer[®] coated with EDTA at 0, 1, 2, 4, 5, 6, 8 and 24 h for the orally administered group and 5, 30 min, 1, 2, 6, 8 and 24 h following IV administration. The blood samples were centrifuged at 14,000 rpm ($14\ 463 \times g$) for 10 min and the supernatant (plasma) was transferred in normal microcentrifuge tubes and stored at -20°C until further analyses were carried out.

Analyses of plasma and tissue samples

The concentrations of AmpB in the plasma and tissue were analyzed according to a developed HPLC method. Prior to analysis, a 100 μ L aliquot of plasma sample was deproteinized using 100 μ L of methanol containing 13.34 μ g/mL of 1-amino 4-nitronaphthalene (IS). The mixture was vortex-mixed for 5 min and then centrifuged at 14,000 rpm ($14\ 463 \times g$) for 10 min. 50 μ L of the supernatant was then injected into the HPLC system.

At predetermined time post administration, the rats were humanely sacrificed and the stomach, small intestine, liver, kidney and spleen were removed after abdominal incision. The organs were pat-dried with laboratory tissue roll, weighed and homogenized using a high speed homogenizer (Ultra-Turrax T-25, Germany) at 24,000 rpm for 8 min under ice with PBS (pH 7.4) making up tissue concentration of 0.25 g/mL. The mixture was further ultrasonicated at 20% amplitude for 8 min. A 100 μ L aliquot of tissue homogenate was mixed with 400 μ L of methanol containing IS (9.09 μ g/mL).

The mixture was vortex-mixed for 5 min and centrifuged at 14,000 rpm ($14\,463 \times g$) for 10 min and 50 μL of the supernatant was injected onto the HPLC system.

Data analyses

The pharmacokinetic parameters were calculated based on a non-compartmental model. Peak concentration (C_{max}) and time of peak concentration (T_{max}) were obtained directly from the individual plasma concentration-time profiles. The T_{lag} referred to the lag time to the appearance of AmpB in the blood after administration. The area under the curve from time zero to last measurable concentration (AUC_{0-t}) was calculated using trapezoidal method. The AUC from the last measurable concentration (C_t) to infinity ($AUC_{t-\infty}$) was calculated by dividing the C_t by k , the apparent elimination rate constant, which in turn was obtained from the terminal slope of the individual plasma concentration-time profiles after logarithmic transformation of the plasma concentration values and application of linear regression. Thus the total ($AUC_{0-\infty}$) was computed as:

$$AUC_{0-\infty} = AUC_{0-t} + C_t/k \quad (1)$$

The MRT was estimated as follows:

$$MRT = AUMC_{0-\infty}/AUC_{0-\infty} \quad (2)$$

where, $AUMC_{0-\infty}$ is area under the first moment versus time curve which is calculated by adding the total area from time zero to the last measurable concentration ($AUMC_{0-t}$) to the area from the last measurable concentration to time infinity ($AUMC_{t-\infty}$) of the plasma concentration times time versus time curves. $AUMC_{0-t}$ was determined using trapezoidal formula while $AUMC_{t-\infty}$ was calculated by dividing the last concentration times time value with elimination rate constant, k .

The MAT was estimated as follows:

$$MAT = MRT_{\text{PO}} - MRT_{\text{IV}} \quad (3)$$

where, MRT is the mean residence time, PO is orally administered formulations and IV refers to administered intravenously.

The absolute bioavailability, F was calculated as below:

$$F = \frac{AUC_{\text{PO}} \cdot \text{Dose}_{\text{IV}}}{AUC_{\text{IV}} \cdot \text{Dose}_{\text{PO}}} 100 \quad (4)$$

where, AUC is the area under the plasma concentration versus time curve from time zero to infinity, PO is the oral administration and IV is the intravenous administration.

The relative bioavailability, F_r was calculated as below:

$$F_r = \frac{AUC_{\text{NLC}}}{AUC_{\text{PO}}} 100 \quad (5)$$

where, AUC_{NLC} is the area under the curve of plasma concentration versus time curve from time zero to infinity of rats administered AmpB NLC or ChiAmpB NLC

orally and AUC_{PO} is the area under the curve of plasma concentration versus time curve from time zero to infinity of rats administered Amphotret[®] orally.

Statistical analyses

Statistical evaluation on samples was performed using a one-way analysis of variance (ANOVA) followed by an independent t-test, where differences were considered significant when $p < 0.05$. Linearity was evaluated by linear regression analysis, which was calculated by least squares regression analysis and the ANOVA test. All calculations were conducted using IBM SPSS Statistics 24 (IBM cooperation, New York, NY).

Results and discussion

Prior to the *in vivo* studies, a HPLC analysis for AmpB in spiked plasma and tissue homogenates was developed and validated. The validity of the assay was verified by linear ANOVA regression analysis, which demonstrated a 95% confidence level in predicting the outcome ($p < 0.05$). All the r^2 values were 0.996 and above, confirming the linearity of the method over the concentrations analyzed (Table 1). The LOD and LOQ values in plasma samples were 0.0093 and 0.031 $\mu\text{g/mL}$ respectively, which are comparably more sensitive than in other studies [20–22]. The LOD in the tissue samples were found to be 0.65 ng/g for liver, 0.97 ng/g for kidney, 0.99 ng/g for spleen, 0.95 ng/g for stomach and 0.87 ng/g for small intestine, are comparatively lower than reported analytical thresholds for AmpB, suggesting a higher sensitivity [1,23].

From Table 2, the average recoveries of AmpB from the biological samples were more than 80%, indicative of an efficient extraction procedure [24]. High percentage of accuracies were observed in plasma samples, 94–97% (Table 2) and are in accordance with other reported values [21,22]. The degree of repeatability was evaluated based on the percentage of coefficient variation (CV) as illustrated in Table 2. The repeatability (CV) of the method in plasma was between 1.77 and 5.89% which are well below the accepted limit of 15% [23,25]. Thus, the developed HPLC method was found to be accurate and reproducible and hence suitable for evaluation of AmpB concentration in rat tissue.

In the present study, four formulations of AmpB (orally administered AmpB NLC, ChiAmpB NLC, Amphotret[®] (PO) and intravenously administered Amphotret[®] (IV)) were administered to either of one of the four groups of Sprague Dawley rats. Sprague Dawley rats were chosen as the animal model in this study due to

Table 1. Linearity evaluation and sensitivity data of AmpB spiked in different biological samples.

	Equation	r^2	LOD	LOQ
Plasma	$y = 0.8769x - 0.0731$	0.9962*	0.0093	0.031
Liver	$y = 0.0324x + 0.0012$	1*	0.65	2.16
Kidney	$y = 0.0293x + 0.0412$	0.9969*	0.97	3.23
Spleen	$y = 0.0341x + 0.0109$	1*	0.99	3.32
Stomach	$y = 0.0394x + 0.0079$	0.9998*	0.95	3.17
Small intestine	$y = 0.0306x + 0.0362$	0.9989*	0.87	2.88

r^2 is the determination coefficient, LOD is the limit of detection and LOQ is the limit of quantification. LOD and LOQ of plasma is in $\mu\text{g/mL}$ while for tissue homogenate are in ng/g.

* $p < 0.05$: statistical significance between the mean peak areas of AmpB/IS and concentration of AmpB.

Table 2. Percentage of recovery, accuracy and precision of AmpB/ IS spiked with plasma and tissue homogenates (mean \pm S.D., $n = 3$ for recovery and $n = 6$ for accuracy and precision).

		Plasma	Liver	Kidney	Spleen	Stomach	Small intestine
Recovery (%)	Low	98.2 \pm 7.0	73.5 \pm 1.4	77.6 \pm 5.1	81.6 \pm 0.3	95.3 \pm 1.6	78.1 \pm 0.7
	Medium	100.0 \pm 0.1	76.1 \pm 1.0	81.2 \pm 0.5	85.0 \pm 0.7	100.2 \pm 0.8	85.0 \pm 0.3
	High	108.5 \pm 1.1	92.8 \pm 1.8	83.5 \pm 0.1	97.9 \pm 0.2	113.7 \pm 0.3	87.6 \pm 0.1
Accuracy (%)	Low	94.4 \pm 2.8	94.8 \pm 1.1	100.3 \pm 5.1	100.4 \pm 0.9	91.8 \pm 1.7	98.9 \pm 0.4
	Medium	97.1 \pm 1.2	99.2 \pm 0.7	97.4 \pm 0.5	97.2 \pm 1.2	93.4 \pm 0.4	98.6 \pm 0.4
	High	94.6 \pm 1.2	97.1 \pm 0.4	96.3 \pm 0.3	95.3 \pm 0.3	94.8 \pm 0.2	98.6 \pm 0.2
Precision (% CV)	Low	5.89	3.24	5.27	0.64	4.93	0.89
	Medium	1.77	1.06	1.52	1.83	3.77	0.87
	High	3.20	2.05	2.07	2.67	2.96	0.80

Low refers to 0.1 μ g/ml in plasma and 2.5 μ g/g in tissue samples; medium refers to 1 μ g/ml in plasma and 10 μ g/g in tissue samples and high refers to 10 μ g/ml in plasma and 100 μ g/g in tissue samples.

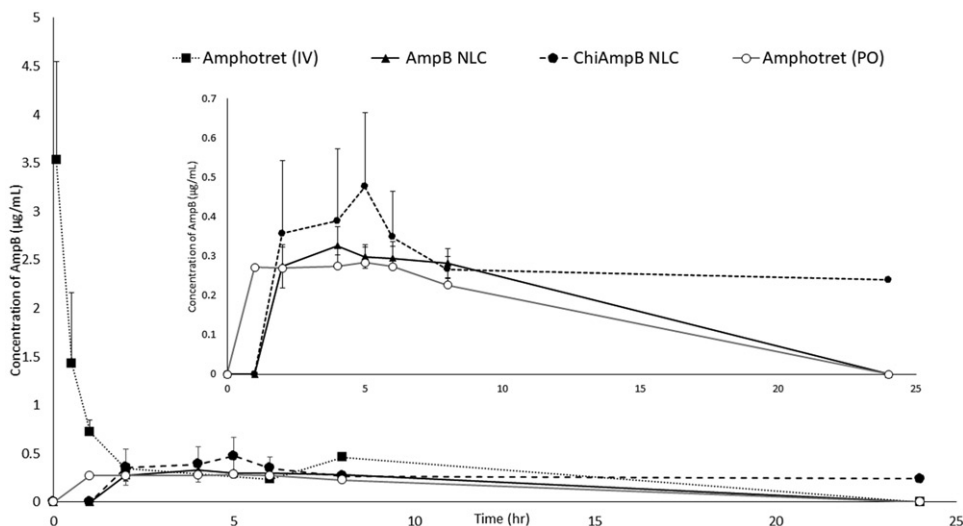


Figure 1. Plasma concentration-time profile of formulations (mean \pm S.D., $n = 3$), $n = 2$ for the 24-hour time point. Insert is the plasma concentration-time profiles of orally administered formulations.

anatomical, physiological, drug absorption profile and expression of transporter enzyme similarities of its intestines to that of the human [26]. The plasma concentration-time profiles following the four-way administration to the rats are depicted in Figure 1 while pharmacokinetic parameters derived from them are shown in Table 3. Upon administration of ChiAmpB NLC formulation, the plasma concentration of AmpB was detectable up to 24h whereas, for the other formulations, it was only detectable up to 8-hour post-administration. As expected, the intravenously administered Amphotret[®] showed a drastic (10-fold) drop in AmpB plasma concentration, from 3.53 ± 1.01 to $0.34 \pm 0.2 \mu$ g/mL 2-hour post administration. This is consistent with the results reported in the literature [27,28].

Orally administered AmpB NLC and ChiAmpB NLC observed lag times (T_{lag}) of 2 h (Figure 1), suggesting that there was a delay in the absorption of both formulations in contrast to Amphotret[®] (PO). We hypothesize that due to their lipidic characteristics, the observed lag times were due to the uptake process *via* lymph, prompted by the mucoadhesive properties of the formulations (particularly ChiAmpB

Table 3. Pharmacokinetic parameters of AmpB from the different formulations (mean \pm S.D., $n = 3$).

Pharmacokinetics parameters	Formulations			
	AmpB NLC	ChiAmpB NLC	Amphotret [®]	Amphotret [®]
Route	Oral	Oral	Oral	IV
Dose (mg/kg)	15	15	15	1
T _{max} (hr)	4.67 \pm 1.15	6.33 \pm 1.52	3.63 \pm 0.29	–
C _{max} (μ g/mL)	0.34 \pm 0.03	0.40 \pm 0.19	0.31 \pm 0.04	–
AUC _{0-∞} (μ g.hr/mL)	27.86 \pm 0.99	34.25 \pm 4.19	14.52 \pm 1.87 ^a	15.97 \pm 1.70
MRT (hr)	7.48 \pm 0.67	21.61 \pm 0.71 ^b	7.51 \pm 0.15	6.00 \pm 0.71
MAT (hr)	1.47 \pm 0.67	15.61 \pm 0.71	1.50 \pm 0.15	–
Absolute F (%)	11.63 \pm 0.41	14.30 \pm 1.74	6.06 \pm 0.78	–
Relative F _r (%)	191.86 \pm 6.82	235.87 \pm 28.85	–	–

T_{max}: time to maximum plasma concentration, C_{max}: maximum plasma concentration, AUC_{0-∞}: area under the curve up to infinity, MRT: mean residence time, MAT: mean absorption time, F: absolute bioavailability and F_r: relative bioavailability.

^a $p < 0.05$: statistical significance between.

^aAmphotret[®] and developed formulations.

^bChiAmpB NLC and the remaining formulations.

NLC) in contrast to Amphotret[®] (PO) formulation as observed in other studies [12,29]. It is normal to observe a lag time of up to 3 h before a noticeable increase in concentration of lipids in lymph or plasma as observed in human [30], rats [31] and sheep [32].

There was a gradual increase in the plasma concentration of AmpB, reaching peak concentration (T_{max}) at approximately 3.6 and 4.7 h, respectively for orally administered Amphotret[®] and AmpB NLC formulations (Table 3). As compared to AmpB NLC, ChiAmpB NLC showed an additional delay of approximately 1.6 h before attaining the T_{max}. The longer T_{max} exhibited by both NLCs formulations may yet affirm the indirect transport of the NLCs into the systemic circulation which is in consistent with results observed by vinpocetine-loaded NLCs [33]. The estimation of T_{max} is dependent on the frequency of blood sampling which was a constraint in the present study due to the limitation and impracticability of frequent sampling points in small rodents like rats. Hence, further interpretation of the data was sought through arithmetic calculation using statistical moment analysis in order to evaluate their MRTs.

MRT refers to the duration of residence of the nanoparticles in the body before elimination. This involves a composite of kinetic processes such as rate and extent of the absorption process, *in vivo* release of AmpB and the distribution of the AmpB to various part of the body [34]. The MRT of ChiAmpB NLC was 21.61 \pm 0.71 hr, which is significantly higher than the Amphotret[®] (PO), 7.51 \pm 0.15 hr ($p < 0.05$) and AmpB NLC, 7.48 \pm 0.67 hr. This suggests that the ChiAmpB NLC remained in the body longer which is attributable to the mucoadhesive properties of the chitosan coating. The mucoadhesiveness of ChiAmpB NLC prolonged the GI transit of the particles through retention at the site of absorption/uptake as well as a slow, sustained release of AmpB which in concert with our previous studies [4,14].

ChiAmpB NLC showed a higher peak plasma concentration (C_{max}), 0.40 \pm 0.19 μ g/mL as compared to AmpB NLC and Amphotret[®] (PO), observing C_{max} of 0.34 \pm 0.03 and 0.31 \pm 0.04 μ g/mL, respectively. Besides, ChiAmpB NLC formulation also observed a significantly higher AUC_{0-∞} ($p < 0.05$) as compared to Amphotret[®] (PO).

The $AUC_{0-\infty}$ of AmpB NLC was significantly higher than Amphotret[®] (PO) ($p < 0.05$) but was not significantly different from ChiAmpB NLC even though the latter observed a higher $AUC_{0-\infty}$. This is in accordance with other studies [4,12] and suggests that the AmpB was better absorbed from ChiAmpB NLC than from uncoated AmpB NLC and Amphotret[®] (PO), which this was also evident in the relative bioavailability (F_r) of ChiAmpB NLC, which was twice higher than Amphotret[®] (PO).

The higher bioavailability observed by both AmpB NLC and ChiAmpB NLC compared to the other orally administered AmpB can be explained by the fact that beeswax and coconut oil promoted the lymphatic transport of the NLCs *via* uptake by the M-cells overlying the lymphoid follicles and Peyer's patches [35,36]. This is supported by studies which showed that the oral absorption of the poorly soluble drugs was enhanced with co-administration with lipids whereby the lymphatic pathway plays a crucial role [12,37]. Studies by Yuan et al. [37] showed that up to 77.9% of lipid nanoparticles were absorbed through the lymphatic pathway while the remaining was transported *via* the portal blood vein. With the lymphatic intestinal pathway, the first pass metabolism in the liver was avoided and thus, bioavailability of the drug was improved.

The incorporation of chitosan coating on the surface of the NLCs is perceived to protect AmpB from the harsh GI environment and thus promotes the uptake by the intestinal lymphatics. Due to the positive charge rendition of chitosan in ChiAmpB NLCs, the NLCs promotes penetration into the negatively charged mucosal layer and through this adhesion, the AmpB was slowly released from the system [14]. Thus, the increase in residence time and intimate contact of the chitosan-coated NLC with the wall of the small intestine provided the requisite for improved AmpB absorption. This is in agreement with findings that there was an enhancement in the uptake of chitosan-coated nanospheres by the gut tissue [4,38]. Furthermore, other drug compounds such as insulin [39], ferrous sulphate [40] and doxorubicin [41] also showed improvement in the respective absorptions through the incorporation of chitosan coating to lipid nanoparticles. Positively charged nanoparticles improved the bioavailability of cyclosporine A in dogs [42] and progesterone in rats [43].

As mucoadhesion was believed to be a prerequisite for the improved bioavailability of the AmpB, further investigation on the amount of AmpB in stomach and the small intestine over the GI transit course of the NLCs was conducted. After 6 h, most of the AmpB from AmpB NLC was found in the small intestine ($73.1 \pm 0.2 \mu\text{g/g}$) whereas the AmpB from ChiAmpB NLC was predominantly found in the stomach ($15.4 \pm 0.1 \mu\text{g/g}$) (Figure 2). AmpB was undetectable in the stomach after 24 h which suggests that all the formulations had emptied into the small intestine by this time. However, AmpB remained detectable in the small intestine of the rats treated with AmpB NLC and ChiAmpB NLC formulations 24-hour post administration which suggest that the GI transit for both formulations were more than 24 h in contrast to the normal reported rats GI transit time of 12–16 h [44,45]. A significant drop ($p < 0.05$) in the concentration of AmpB was observed in the intestinal tissue in rats treated with AmpB NLC, from 73.1 ± 0.2 to $10.2 \pm 0.4 \mu\text{g/g}$ between 6 to 8-hour post administration, respectively. A further drop in the concentration was observed from AmpB NLC between 8 and 24-hour post administration, reaching a final

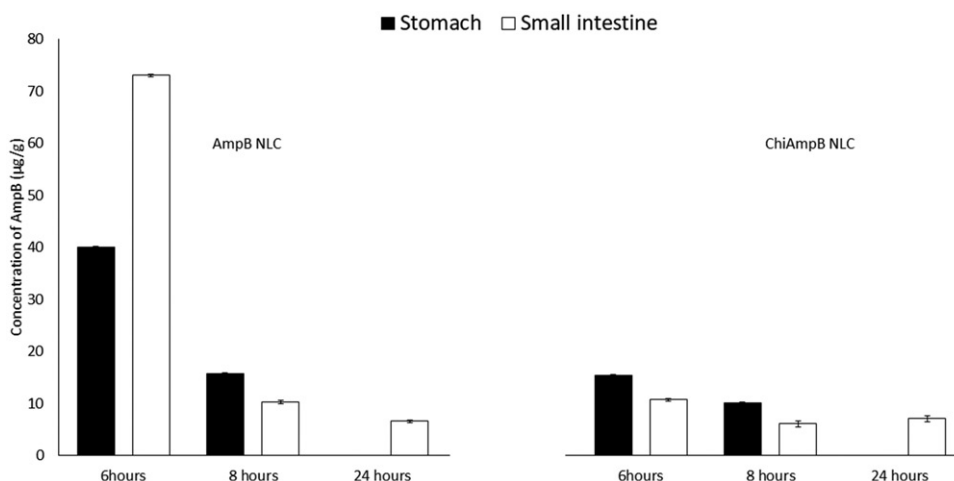


Figure 2. Concentration of AmpB in stomach and small intestine over 6–24 h-post administration (mean \pm S.D., $n = 3$), * $p < 0.05$: statistical significance between 6 and 8-hour values.

concentration of $6.6 \pm 0.3 \mu\text{g/g}$ (Figure 2). It is interesting to note that AmpB NLCs was detectable in the small intestine 24-hour post administration which can be explained by the small size dimensions of AmpB NLCs with a concomitant increase in surface area, which together, enhanced the interactive forces at play during mucoadhesion [11,13].

On the other hand, the ChiAmpB NLC observed only minimal changes to the concentration of AmpB in the small intestine, with differences of about 4.6 and 1.0 $\mu\text{g/g}$ between 6–8 h and 8–24 h. Furthermore, ChiAmpB NLC observed a higher concentration of AmpB ($7.1 \pm 0.6 \mu\text{g/g}$) post 24-hour administration as compared to AmpB NLC, believed to be due to additional mucoadhesive power provided by the chitosan coating. The preceding accords well with the results from the pharmacokinetics studies (Table 3), in which ChiAmpB NLC recorded a longer MAT compared to AmpB NLC, attributable to prolong residence time of the particles at the absorption site.

One of the major limitations to the clinical applications of the AmpB is its nephrotoxicity. Figure 3 show that Amphotret[®] (IV) marked a five-fold higher accumulation of AmpB in the kidneys in contrast to ChiAmpB NLC at 8-hour post administration. On the other hand, ChiAmpB NLC showed the lowest renal disposition at $4.0 \pm 0.9 \mu\text{g/g}$ followed by AmpB NLC and Amphotret[®] (PO), at 5.1 ± 0.2 and $5.9 \pm 1.4 \mu\text{g/g}$, respectively. Amphotret[®] (IV) continued to show preferential disposition in the kidneys 24-hour post administration, significantly ($p < 0.05$) higher than from ChiAmpB NLC and AmpB NLC formulations. This is in accordance with reports which showed that Amphotret[®] (IV) was more nephrotoxic than orally administered lipid-based formulations of AmpB [1,12].

We believe that the observed difference in the renal disposition of AmpB was due to the aggregation states of AmpB whereby, Amphotret[®] exhibited the dimer configuration whilst AmpB in the NLCs formulations exhibited the polyaggregate states [13]. Studies by Espada et al. [46] revealed that the dimer state of AmpB showed preferential disposition in the kidneys and observed mostly, unilateral kidney

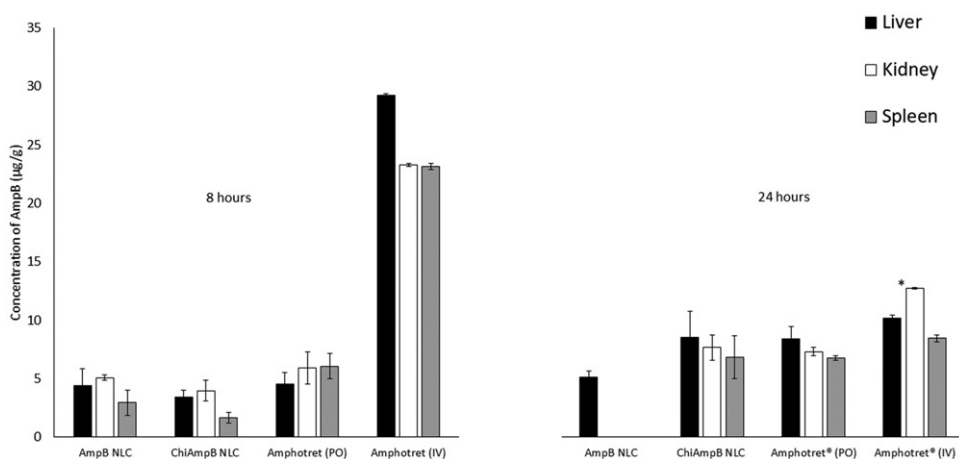


Figure 3. Tissue distribution of AmpB in rats administered with different formulations over time (mean \pm S.D., $n = 3$), * $p < 0.05$: statistical significance between Amphotret®(IV) and ChiAmpB NLC as well as AmpB NLC formulations.

atrophy in mice while the polyaggregate states of AmpB conserved both kidneys with a normal size and appearance. Based on these results, it is likely that the low renal tissue levels of AmpB in rats treated with ChiAmpB NLC may demonstrate a lower nephrotoxicity potential and thus, may establish a safer toxicity profile than current marketed formulations [3].

The liver and spleen are part of the RES organs which are target organs for fungal infections as well as intracellular parasites of *Leishmaniasis* genus [27]. IV administration of Amphotret® to rats registered the highest concentration of AmpB in both liver and spleen, followed by oral administration of Amphotret®, AmpB NLC and ChiAmpB NLC 8-hour post administration (Figure 3). The possible reason for this phenomenon has to do with the high blood perfusion to these organs and/or the high uptake of the cells in the RES-type organs [47].

However, the clearance of AmpB from liver and spleen was faster in rats treated with Amphotret® (IV), falling drastically to 10.2 ± 0.2 and 8.4 ± 0.3 $\mu\text{g/g}$ in liver and spleen, respectively 24-hour post administration. This indicates that the uptake of the Amphotret® (IV) by the RES cells was not significant [47]. On the other hand, a three-fold increase in AmpB accumulation in both liver and spleen following administration of ChiAmpB NLC was observed at 24 h. This is in contrast to the uncoated AmpB NLC, which showed undetectable amount of AmpB in the spleen. The presence of a high AmpB deposition in the liver and spleen in rats administered with ChiAmpB NLC serves the possibility of utilizing the former in visceral *Leishmaniasis*.

Conclusion

In summary, ChiAmpB NLC demonstrated an improvement in the oral bioavailability of AmpB compared to the uncoated AmpB NLC and Amphotret® (delivered orally or intravenously). This improved bioavailability appears to be a culmination of factors including prolonged retention of ChiAmpB NLC within the small intestine,

absorption *via* intestinal lymphatic pathway, hence avoidance of first hepatic clearance and a slow, sustained release of AmpB from ChiAmpB NLC. Furthermore, the ChiAmpB NLC presents a lower risk for nephrotoxicity and higher accumulation in the liver and spleen. Thus, not only have the limitations inherent with the current mode of AmpB administration been addressed but also, a clinical targeted strategy is a possibility in the treatment of visceral leishmaniasis.

Disclosure statement

No potential conflict of interest was reported by the author(s).

ORCID

Clive Roberts  <http://orcid.org/0000-0001-9443-3445>

Nashiru Billa  <http://orcid.org/0000-0002-8496-1882>

References

- [1] Gershkovich P, Wasan EK, Lin M, et al. Pharmacokinetics and biodistribution of amphotericin B in rats following oral administration in a novel lipid-based formulation. *J Antimicrob Chemother.* 2009;64(1):101–108.
- [2] Jain V, Gupta A, Pawar VK, et al. Chitosan-assisted immunotherapy for intervention of experimental leishmaniasis via amphotericin B-loaded solid lipid nanoparticles. *Appl Biochem Biotechnol.* 2014;174(4):1309–1330.
- [3] Chaudhari MB, Desai PP, Patel PA, et al. Solid lipid nanoparticles of amphotericin B (AmbiOnp): in vitro and in vivo assessment towards safe and effective oral treatment module. *Drug Deliv Transl Res.* 2016;6(4):354–364.
- [4] Jabri T, Imran M, Shafiullah, et al. Fabrication of lecithin-gum tragacanth muco-adhesive hybrid nano-carrier system for in-vivo performance of amphotericin B. *Carbohydr Polym.* 2018;194:89–96.
- [5] Yang Z, Tan Y, Chen M, et al. Development of amphotericin B-loaded cubosomes through the SolEmuls technology for enhancing the oral bioavailability. *AAPS PharmSciTech.* 2012;13(4):1483–1491.
- [6] Amekyeh H, Billa N, Yuen K, et al. A gastrointestinal transit study on amphotericin B-loaded solid lipid nanoparticles in rats. *AAPS PharmSciTech.* 2015;16(4):871–877.
- [7] Halde C, Newcomer VD, Wright ET, et al. An evaluation of amphotericin B in vitro and in vivo in mice against *Coccidioides immitis* and *Candida albicans*, and preliminary observations concerning the administration of amphotericin B to man. *J Invest Dermatol.* 1957;28(3):217–232.
- [8] Serrano DR, Lalatsa A, Dea-Ayuela MA, et al. Oral particle uptake and organ targeting drives the activity of amphotericin B nanoparticles. *Mol Pharmaceutics.* 2015;12(2):420–431.
- [9] Paliwal R, Rai S, Vaidya B, et al. Effect of lipid core material on characteristics of solid lipid nanoparticles designed for oral lymphatic delivery. *Nanomedicine* 2009;5(2):184–191.
- [10] Cai S, Yang Q, Bagby TR, et al. Lymphatic drug delivery using engineered liposomes and solid lipid nanoparticles. *Adv Drug Deliv Rev.* 2011;63(10-11):901–908.
- [11] Khosa A, Reddi S, Saha RN. Nanostructured lipid carriers for site-specific drug delivery. *Biomed Pharmacother.* 2018;103:598–613.
- [12] Sachs-Barrable K, Lee SD, Wasan EK, et al. Enhancing drug absorption using lipids: a case study presenting the development and pharmacological evaluation of a novel lipid-

- based oral amphotericin B formulation for the treatment of systemic fungal infections. *Adv Drug Deliv Rev.* 2008;60(6):692–701.
- [13] Tan SLJ, Roberts CJ, Billa N. Mucoadhesive chitosan-coated nanostructured lipid carriers for oral delivery of amphotericin B. *Pharm Dev Technol.* 2019;24(4):504–512.
- [14] Tan SLJ, Roberts CJ, Billa N. Antifungal and mucoadhesive properties of an orally administered chitosan-coated amphotericin B nanostructured lipid carrier (NLC). *AAPS PharmSciTech.* 2019;20(136):1–11.
- [15] Serrano DR, Lalatsa A. Oral amphotericin B: the journey from bench to market. *J Drug Deliv Sci Technol* 2017;42:1–9.
- [16] Torrado JJ, Espada R, Ballesteros MP, et al. Amphotericin B formulations and drug targeting. *J Pharm Sci.* 2008;97(7):2405–2425.
- [17] Torrado JJ, Serrano DR, Uchegbu IF. The oral delivery of amphotericin B. *Ther Deliv.* 2013;4(1):9–12.
- [18] Jain S, Valvi PU, Swarnakar NK, et al. Gelatin coated hybrid lipid nanoparticles for oral delivery of amphotericin B. *Mol Pharmaceutics.* 2012;9(9):2542–2553.
- [19] Caldeira LR, Fernandes FR, Costa DF, et al. Nanoemulsions loaded with amphotericin B: a new approach for the treatment of leishmaniasis. *Eur J Pharm Sci.* 2015;70:125–131.
- [20] Espada R, Josa JM, Valdespina S, et al. HPLC assay for determination of amphotericin B in biological samples. *Biomed Chromatogr.* 2008;1(22):402–407.
- [21] Italia JL, Singh D, Ravi Kumar M. High-performance liquid chromatographic analysis of amphotericin B in rat plasma using alpha-naphthol as an internal standard. *Anal Chim Acta.* 2009;634(1):110–114.
- [22] Chakrabarty US, Pal TK. Rapid and sensitive high performance liquid chromatography method for the determination of amphotericin B in rat plasma. *J Pharm Res* 2011;4(9):3194–3197.
- [23] Echevarría I, Barturen C, Renedo MJ, et al. High-performance liquid chromatographic determination of amphotericin B in plasma and tissue. Application to pharmacokinetic and tissue distribution studies in rats. *J Chromatogr.* 1998;819:171–176.
- [24] Colombo M, Melchiades GL, Figueiró F, et al. Validation of an HPLC-UV method for analysis of kaempferol-loaded nanoemulsion and its application to in vitro and in vivo tests. *J Pharm Biomed Anal.* 2017;145:831–837.
- [25] Campanero MA, Zamarrefio AM, Diaz M, et al. Development and validation of an HPLC Method for determination of amphotericin B in plasma and sputum Involving solid phase extraction. 1997;46:641–646.
- [26] Cao X, Gibbs ST, Fang L, et al. Why is it challenging to predict intestinal drug absorption and oral bioavailability in human using rat model. *Pharm Res.* 2006;23(8):1675–1686.
- [27] Echevarria I, Barturen C, Renedo MJ, et al. Comparative pharmacokinetics, tissue distributions, and effects on renal function of novel polymeric formulations of amphotericin B and amphotericin B-deoxycholate in rats. *Antimicrob Agents Chemother.* 2000;44(4):898–904.
- [28] Jung SH, Lim DH, Jung SH, et al. Amphotericin B-entrapping lipid nanoparticles and their in vitro and in vivo characteristics. *Eur J Pharm Sci.* 2009;37(3-4):313–320.
- [29] Brocks DR, Davies NM. Lymphatic drug absorption via the enterocytes: pharmacokinetic simulation, modeling, and considerations for optimal drug development. *J Pharm Pharm Sci.* 2018;21(1s):254s–2570.
- [30] Cohn JS, Johnson EJ, Millar JS, et al. Contribution of apoB-48 and apoB-100 triglyceride-rich lipoproteins (TRL) to postprandial increases in the plasma concentration of TRL triglycerides and retinyl esters. *J Lipid Res.* 1993;34(12):2033–2040.
- [31] Trevasakis NL, Hu L, Caliph SM, et al. The mesenteric lymph duct cannulated rat model: application to the assessment of intestinal lymphatic drug transport. *J Vis Exp.* 2015;9:1–11.

- [32] Windmueller HG, Spaeth AE. Fat transport and lymph and plasma lipoprotein biosynthesis by isolated intestine. *J Lipid Res.* 1972;13(1):92–105.
- [33] Zhuang C, Li N, Wang M, et al. Preparation and characterization of vinpocetine loaded nanostructured lipid carriers (NLC) for improved oral bioavailability. *Int J Pharm.* 2010;394(1–2):179–185.
- [34] De B, Bhandari K, Chakravorty N, et al. Computational pharmacokinetics and in vitro-in vivo correlation of anti-diabetic synergistic phyto-composite blend. *WJD.* 2015;6(11):1179–1185.
- [35] Hussain N, Jaitley V, Florence AT. Recent advances in the understanding of uptake of microparticulates across the gastrointestinal lymphatics. *Adv Drug Deliv Rev.* 2001;50(1–2):107–142.
- [36] Yuan Y, Li YB, Tai ZF, et al. Study of forced degradation behavior of pramlintide acetate by HPLC and LC-MS. *J Food Drug Anal.* 2018;26(1):409–415.
- [37] Yuan H, Chen J, Du Y, et al. Studies on oral absorption of stearic acid SLN by a novel fluorometric method. *Colloids Surf B Biointerfaces.* 2007;58(2):157–164.
- [38] Takeuchi H, Yamamoto H, Kawashima Y. Mucoadhesive nanoparticulate systems for peptide drug delivery. *Adv Drug Deliv Rev.* 2001;47(1):39–54.
- [39] Fonte P, Andrade F, Araújo F, et al. Chitosan-coated solid lipid nanoparticles for insulin delivery. *Meth Enzymol.* 2012;508:295–314.
- [40] Zariwala MG, Elsaid N, Jackson TL, et al. A novel approach to oral iron delivery using ferrous sulphate loaded solid lipid nanoparticles. *Int J Pharm.* 2013;456(2):400–407.
- [41] Ying XY, Cui D, Yu L, et al. Solid lipid nanoparticles modified with chitosan oligosaccharides for the controlled release of doxorubicin. *Carbohydr Polym.* 2011;84(4):1357–1364.
- [42] El-Shabouri M. Positively charged nanoparticles for improving the oral bioavailability of cyclosporin-A. *Int J Pharm.* 2002;249(1-2):101–108.
- [43] Gershanik T, Benita S. Positively charged self-emulsifying oil formulation for improving oral bioavailability of progesterone. *Pharm Dev Techn.* 1996;1(2):147–157.
- [44] Padmanabhan P, Grosse J, Asad A, et al. Gastrointestinal transit measurements in mice with ^{99m}Tc-DTPA-labeled activated charcoal using NanoSPECT-CT. *EJNMMI Res.* 2013;3(1):60–68.
- [45] Dalziel JE, Young W, Bercik P, et al. Tracking gastrointestinal transit of solids in aged rats as pharmacological models of chronic dysmotility. *Neurogastroenterol Motil.* 2016;28(8):1241–1251.
- [46] Espada R, Valdespina S, Dea MA, et al. In vivo distribution and therapeutic efficacy of a novel amphotericin B poly-aggregated formulation. *J Antimicrob Chemother.* 2008;61(5):1125–1131.
- [47] Banerjee T, Mitra S, Kumar Singh A, et al. Preparation, characterization and biodistribution of ultrafine chitosan nanoparticles. *Int J Pharm.* 2002;243(1-2):93–105.